

Z. Ahmed, L.S. Nasrat, M. Rihan

The effect of SiO₂ microparticle concentration on the electrical and thermal properties of silicone rubber for electrical insulation applications

Introduction. Polymeric insulators, first developed in the 1950s, have since seen substantial advancements in both design and manufacturing, making them increasingly appealing to users and manufacturers in the electrical industry. Extensive testing in both laboratory and outdoor environments has consistently demonstrated that polymeric insulators outperform traditional porcelain and glass counterparts. Among the various polymeric materials, silicone rubber (SiR) has emerged as one of the most promising candidates for high-voltage insulators. Its superiority is attributed to a unique combination of properties, including a non-conductive chemical structure, high dielectric strength, and excellent resistance to scaling. To further enhance these properties, SiR is often combined with fillers to form composite materials. These SiR composites are at the forefront of advanced high-voltage insulation systems, offering improved mechanical, thermal, and electrical performance. As a result, they not only meet the rigorous demands of high-voltage applications but also provide a significantly extended service life. **Goal.** This study aims to enhance the dielectric and thermal properties of SiR by incorporating micron-sized silicon dioxide (SiO₂) filler. **Methodology.** SiR-based composite samples were prepared by incorporating micron-sized SiO₂ at weight fractions of 10 %, 20 %, 30 %, and 40 % of the total composition. Initially, the samples were heated to specific temperatures (25°C, 60°C, 80°C, and 100°C) before undergoing dielectric strength testing to evaluate their performance under varying thermal conditions. Additionally, the samples were subjected to thermal aging for durations of 10, 20, and 30 minutes at the same temperatures before dielectric strength assessment. **The results** indicated that increasing the filler concentration enhanced the dielectric strength of the SiR/SiO₂ composites. The highest breakdown voltage was observed at a filler concentration of 30 %. **Practical value.** Incorporating micron-sized SiO₂ filler into the SiR matrix enhanced the composite's resistance to thermal stress. Compared to SiR-based composites with varying SiO₂ concentrations, pure SiR exhibited the lowest dielectric strength. References 48, tables 5, figures 8. **Key words:** dielectric strength, silicone rubber, micron-sized silica dioxide, thermal behavior, neural network.

Вступ. Полімерні ізолятори з моменту розробки в 1950-х роках значно удосконалилися як у проектуванні, так і у виробництві, що робить їх все більш привабливими для користувачів та виробників електротехнічної продукції. Великі випробування як у лабораторних, так і промислових умовах демонструють, що полімерні ізолятори переважають традиційні порцелянові і скляні аналоги. Серед різних полімерних матеріалів силіконовий каучук (SiR) став найперспективнішим матеріалом для високовольтних ізоляторів. Його перевага пояснюється унікальним поєднанням властивостей, включаючи непровідну хімічну структуру, високу діелектричну міцність та відмінну стійкість до утворення накипу. Для подальшого покращення цих властивостей, SiR часто поєднують з наповнювачами для формування композитних матеріалів. Ці композити SiR знаходяться на передньому краї сучасних систем високовольтної ізоляції, пропонуючи покращені механічні, теплові та електричні характеристики. В результаті вони не тільки відповідають жорстким вимогам високовольтних застосувань, а й забезпечують значно більший термін служби. **Метою** дослідження є покращення діелектричних та теплових властивостей SiR шляхом включення наповнювача діоксиду кремнію (SiO₂) мікронного розміру. **Методологія.** Зразки композиту SiR були приготовлені шляхом включення різних вагових відсотків мікронного розміру SiO₂ відповідно 10 %, 20 %, 30 % та 40 % від загальної ваги. Потім діелектрична міцність цих зразків була оцінена за чотирьох температур: 25 °C, 60 °C, 80 °C і 100 °C для оцінки ефективності ефекти в різних умовах. Крім того, зразки старіли протягом 10, 20 і 30 хвилин при тих же температурах перед випробуванням. **Результати** досліджували вплив термічної поведінки на характеристики напруги пробою композитів SiR, зістарених у різний час і за різних температур. Результати показують, що збільшення концентрації наповнювача збільшує діелектричну міцність SiR композитів. Найкраща пробивна напруга досліджених зразків була отримана при концентрації наповнювача 30 %. **Практична цінність.** Додавання наповнювача SiO₂ мікронного розміру в матрицю SiR підвищує опір полімерних композитів термічним механічним напругам. У порівнянні з SiR, завантаженим SiO₂ у різних концентраціях, чистий SiR має найнижчу діелектричну міцність. Бібл. 48, табл. 5, рис. 8.

Ключові слова: діелектрична міцність, силіконова гума, діоксид кремнію мікророзміру, термічна поведінка, нейронна мережа.

Introduction. Electrical insulators are critical components in power systems, ensuring the safe and efficient transmission and distribution of electricity. As power systems evolve to meet increasing demands and integrate renewable energy sources [1–5], the role of insulators becomes even more vital [6–8]. Polymeric materials come in several forms, including high-density polyethylene, silicone rubber (SiR), ethylene propylene diene monomer, and ethylene rubber [9, 10].

Because SiR has several advantages, including high dielectric strength (DS) and scale resistance, it is widely used in electrical applications. However, it is expensive and has poor mechanical strength and tracking resistance [11–14]. Therefore, pure silicone is grafted with some fillers to enhance its mechanical, thermal, and electrical properties and increase its service life; this combination is named SiR composites [15–18]. A composite is a material composed of two or more distinct constituent materials. These constituents exhibit significant differences in their physical and chemical properties compared to the individual components before combination [19].

Fillers like alumina trihydrate, aluminum oxide, zinc oxide, titanium oxide, calcium carbonate, and barium titanate

that are added to SiR have gotten a lot of attention [20–22]. A lot of research has been done on how mixtures of micro- and nanosized fillers affect the mechanical, electrical, and thermal properties of SiR-based composites [23–25]. Developing micro- and nanocomposite materials can enhance the thermal and electrical characteristics [26–31]. The DS of polymers in HV applications is a crucial factor in assessing their dielectric performance [32–35].

Neural networks (NN) are a class of artificial intelligence models that draw inspiration from the design and operation of biological NNs, like those found in the human brain [36]. Because of their effectiveness, speed, and ability to handle complex nonlinear functions, they are frequently used to solve complicated and challenging real-world problems. This technique has been applied in several complicated engineering applications in various fields, including classification, prediction, intricate practical transformation models, and many other domains [37, 38].

The goal of the paper is to improve the SiR's dielectric strength under varying environmental conditions by adding an appropriate weight percentage of

inorganic filler. This work investigates, evaluates, and records the impact of micron-sized silica filler on the electrical and thermal properties of SiR insulators.

The NNs technique has been adopted to define the DS of the unmanufactured samples that have filler ratios in between the filler ratios of the manufactured samples. The goal is to define the DS of the unmanufactured samples, which have filler ratios in between those of the manufactured samples. Samples define the DS of the unmanufactured samples that have filler ratios in between the filler ratios of the manufactured samples.

Materials. In this study, the following chemical components were used:

1. The high-temperature vulcanized solid SiR was supplied by the German Company Sonax. Solid SiR contains high-molecular-weight polymers and relatively long polymer chains.

2. The filler used in this study is silicon dioxide (SiO_2) in micron-sized powder form. Supplied by Nanotech Egypt, it has a particle size of $20 \mu\text{m} \pm 5 \text{nm}$.

Sample preparation. The samples were fabricated in the form of discs with a diameter of 5 cm and a thickness of 2 mm for the DS test. Five different concentrations of SiR/ SiO_2 composites were prepared, as specified in Table 1.

Table 1

Formulations of the prepared SiR/ SiO_2 composite samples

Composite symbol	Mixtures of specimens
B	100 wt. % SiR
S10	90 wt. % SiR + 10 wt. % micron-sized SiO_2
S20	80 wt. % SiR + 20 wt. % micron-sized SiO_2
S30	70 wt. % SiR + 30 wt. % micron-sized SiO_2
S40	60 wt. % SiR + 40 wt. % micron-sized SiO_2

Micron-sized silica filler was added to the SiR base polymer to create the SiR composite samples. Filler concentrations are expressed as a percentage of the base polymer's total weight. The mixture is placed in a two-cylinder mill in the lab, which has a 470 mm diameter, 300 mm of operating distance, and a 1 mm gap between the cylinders. A day was given to the specimens prior to vulcanization. Figure 1 shows the rolling machine that is used for SiR processing. The samples were cut to the dimensions that were most appropriate for each testing procedure. It can be noted that the samples' color changes when SiO_2 filler is added (Fig. 2).

Dielectric strength test, which is a fundamental examination of an insulating material's electrical properties, is measured in voltage per unit length (kV/mm) [6, 39]. It illustrates how the insulating material withstands the intensity of an electric field without changing or losing its insulating properties. The shape of the used samples in the test should be a disc with a 1 mm thickness and a 5 cm diameter. Figure 3 shows the dielectric breakdown strength testing circuit. HV AC is applied to evaluate the breakdown voltage of the tested samples in various situations. To reduce surges on the transformer's HV side and more accurately determine the specimen's breakdown voltage, it is important to remember that the voltage applied to the specimen should be changed gradually and slowly. Because of the importance of the results, the test of each set was repeated many times, the data was gathered with high precision each time, and then the average value of the tested sample for each set was calculated and recorded.

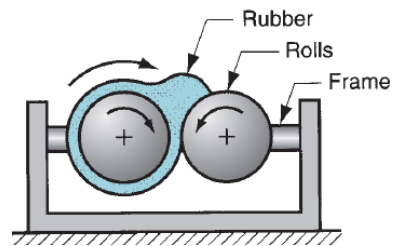


Fig. 1. Rolling machine used for processing SiR samples

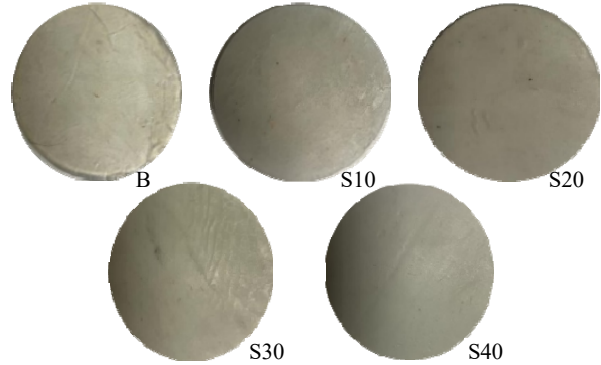


Fig. 2. Images of prepared SiR/ SiO_2 composite samples

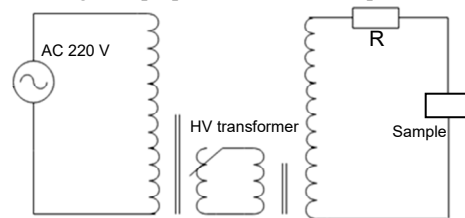


Fig. 3. The dielectric breakdown strength test laboratory circuit

Dielectric strength test procedure. In the testing circuit (Fig. 3), the test cells were energized using a test transformer (220 V / 100 kV) to determine the breakdown strength. The test cells were filled with transformer oil [40]. The DS of composite samples aged under multiple thermal-electrical stresses for different aging durations was evaluated at four temperature levels ranging from 25 °C to 100 °C, categorized as follows.

1) In the first scenario, the studied composite samples were heated until they reached different temperatures (25 °C, 60 °C, 80 °C, and 100 °C) with an initial exposure time of 0 min to these temperatures and then subjected to the DS tests. The first temperature (25 °C) represents normal ambient operating conditions. To simulate short-circuit conditions the temperature was set to 60 °C. The third temperature (80 °C) was selected to represent high-fault conditions under operating voltages exceeding 30 kV. Finally, the fourth temperature (100 °C) was chosen to simulate operation under heavy loading conditions and in environments with elevated temperatures.

2) In the second scenario, the composite samples subjected to thermal stress were analyzed as a function of aging time. They underwent thermal aging for 10, 20, and 30 minutes at the same test temperatures specified in the previous first scenario.

Experimental results and discussion. Dielectric strength results under the first scenario. Figure 4 presents the relationship between DS and the concentration of micro-sized SiO_2 under varying temperatures, evaluated according to the conditions of the first scenario.

At 25 °C, the breakdown voltages of S10, S20, S30, and S40 were 29.93, 34.8, 36.58, and 33.1 kV/mm, respectively. These values were higher than the DS of the pure sample (B), which measured 28.06 kV/mm.

A similar trend was observed at 60 °C, where the DS values of S10, S20, S30, and S40 increased to 27.01, 31.9, 33.02, and 30.47 kV/mm, respectively, surpassing the DS of B (26.21 kV/mm).

At 80 °C, the DS values of S10, S20, S30, and S40 were 24, 28.13, 29.64, and 27.44 kV/mm, respectively, again exceeding the DS of B (22.51 kV/mm).

Finally, at 100 °C, the DS values of S10, S20, S30, and S40 were 18.69, 19.87, 21.3, and 19.42 kV/mm, respectively, demonstrating improved performance compared to the DS of B (16.01 kV/mm).

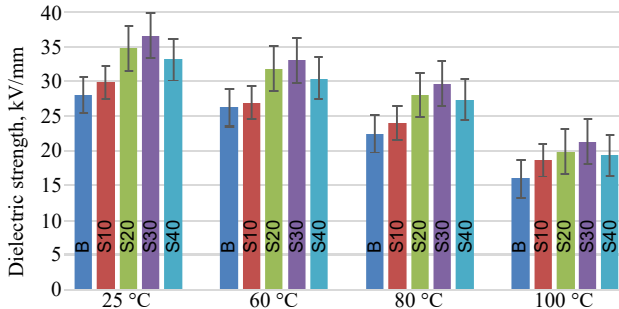


Fig. 4. Dielectric strength of the studied samples evaluated under the conditions of the first scenario

Dielectric strength results under the second scenario. According to the second scenario, additional sets of B, S10, S20, S30, and S40 were subjected to thermal aging at 25 °C, 60 °C, 80 °C, and 100 °C for 10, 20, and 30 minutes before undergoing the DS test.

Effect of 10-minute thermal aging. As shown in Fig. 5, incorporating different concentrations of SiO₂ into the composite samples (S10, S20, S30, and S40) and aging them for 10 minutes at 25 °C resulted in AC DS enhancements of 4 %, 22 %, 28 %, and 16 %, respectively. The corresponding DS values were 27.23, 32.01, 33.65, and 30.59 kV/mm, compared to the pure SiR (B) sample, which exhibited a DS of 26.32 kV/mm.

At 60 °C, the DS values of S10, S20, S30, and S40 increased to 25.27, 29.67, 31.28, and 28.09 kV/mm, respectively, surpassing the DS of B (24.03 kV/mm).

At 80 °C, the DS values of S10, S20, S30, and S40 were 23.84, 24.88, 27.09, and 24.02 kV/mm, respectively, all higher than the DS of B (20.01 kV/mm).

At 100 °C, the DS values of S10, S20, S30, and S40 reached 16.23, 17.00, 19.06, and 15.88 kV/mm, respectively, significantly exceeding the DS of B (12.54 kV/mm).

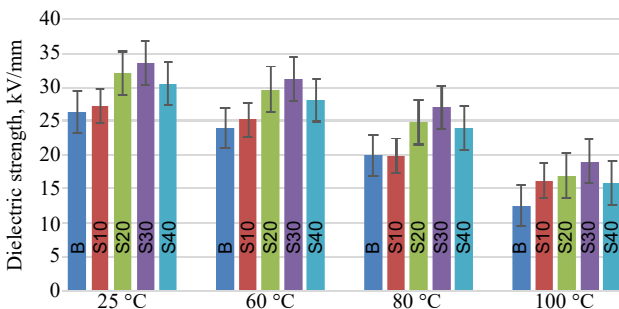


Fig. 5. Effect of 10-minute thermal aging on the dielectric strength of the studied samples

Effect of 20-minute thermal aging. At 25 °C, the DS of the studied samples S10, S20, S30, and S40 improved by

approximately 5 %, 22 %, 30 %, and 18 %, respectively, reaching 26.1, 30.5, 32.39, and 29.37 kV/mm, compared to the DS of the pure SiR (B) sample, which was 25 kV/mm, as illustrated in Fig. 6.

At 60 °C, the DS values of S10, S20, S30, and S40 increased to 21.19, 25.47, 27.77, and 24.78 kV/mm, respectively, compared to sample B (20.44 kV/mm).

At 80 °C, the DS values were further enhanced to 18.89, 19.78, 21.66, and 18.27 kV/mm for S10, S20, S30, and S40, respectively, compared to 15 kV/mm for the B sample.

At 100 °C, the DS values of S10, S20, S30, and S40 were enhanced to 14.02, 15.49, 17.62, and 14.36 kV/mm, respectively, compared to sample B (10 kV/mm).

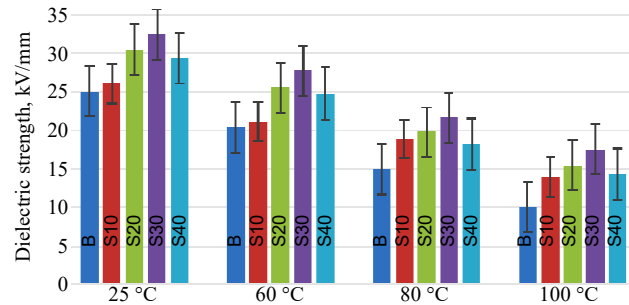


Fig. 6. Effect of 20-minute thermal aging on the dielectric strength of the studied samples

Effect of 30-minute thermal aging. At 25 °C, the DS values of S10, S20, S30, and S40 increased to 22.44, 26.59, 29.00, and 25.09 kV/mm, respectively, compared to the DS of sample B (21.52 kV/mm).

As shown in Fig. 7, comparable improvements were observed at 60 °C, where the DS values of S10, S20, S30, and S40 increased to 20.11, 21.13, 23.09, and 20.45 kV/mm, respectively, while the DS of sample B was 16 kV/mm.

At 80 °C, the DS values of S10, S20, S30, and S40 increased to 17.77, 18.59, 20.59, and 17.30 kV/mm, respectively, compared to 14 kV/mm for sample B.

At 100 °C, the DS values for S10, S20, S30, and S40 improved by 43 %, 60 %, 83 %, and 47 %, respectively, compared to the DS of sample B.

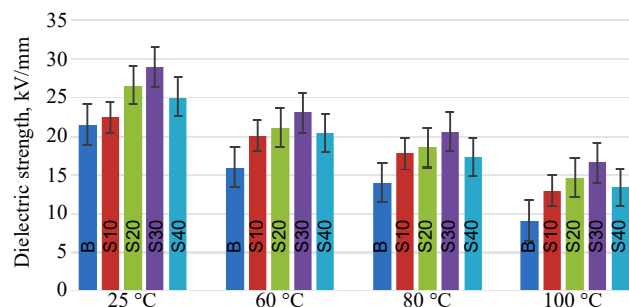


Fig. 7. Effect of 30-minute thermal aging on the dielectric strength of the studied samples

These results confirmed the overall trend observed in AC DS testing: the DS increased with higher SiO₂ filler concentration, peaking at 30 wt %. Beyond this concentration, a decline in DS was observed, likely due to agglomeration or conduction path formation between filler particles. The initial improvement is attributed to the formation of interaction zones within the SiR matrix [41–43].

These zones enhanced the interfacial area, thereby increasing the probability of charge trapping (e.g., electrons) at filler-matrix interfaces, which suppresses carrier mobility and improves breakdown strength [44–46].

Neural network (NN) modeling. An artificial neural network (NN) typically comprises an input layer, one or more hidden layers, and an output layer. Its performance depends on factors such as the number of neurons in each layer [47, 48]. Figure 8 presents the general architecture of the NN used in this study.

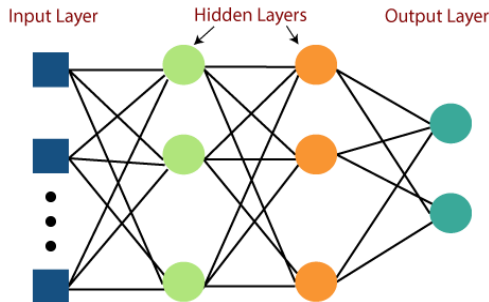


Fig. 8. General structure of a multilayer NN

NN validation in the first scenario application.

Table 2 presents the experimental and NN-predicted DS values of SiR-based composite samples according to the first scenario. Four samples were used for model training, while the fifth sample served as a test case. The NN model demonstrated high prediction accuracy, with error percentages ranging from 0.0033 % (S40 at 80 °C) to 0.0977 % (S20 at 25 °C).

Table 2
Experimental and NN results for the dielectric strength of SiR-based composite samples (first scenario)

Sample	$T, ^\circ\text{C}$	Dielectric strength, kV/mm		
		Experimental results	NN estimations	Error, %
B	25 °C	28.06	28.036	0.0855
S10		29.93	29.9271	0.0097
S20		34.8	34.766	0.0977
S30*		36.58	36.6004	0.0558
S40		33.1	33.1013	0.0039
B		60 °C	26.21	26.2113
S10	27.01		27.0064	0.0133
S20	31.9		31.8902	0.0307
S30*	33.02		33.0178	0.0067
S40	30.47		30.459	0.0361
B	80 °C		22.51	22.4921
S10		24	24.0152	0.0633
S20		28.13	28.1262	0.0135
S30*		29.64	29.6365	0.0118
S40		27.44	27.4409	0.0033
B		100 °C	16.01	16.0142
S10	18.69		18.6777	0.0658
S20	19.87		19.8523	0.0891
S30*	21.3		21.303	0.0141
S40	19.42		19.4027	0.0891

Note: * Indicates samples used for model testing.

NN validation (effect of 10-minute thermal aging). Table 3 summarizes the DS results for the studied samples. Again, the NN model was trained on four samples and tested on the fifth. The prediction error ranged from 0.0015 % (S10 at 25 °C) to 0.1448 % (S40 at 100 °C), validating the model's reliability.

Table 3

Experimental and NN results for the dielectric strength of SiR-based composite samples (effect of 10-minute thermal aging)

Sample	$T, ^\circ\text{C}$	Dielectric strength, kV/mm		
		Experimental results	NN estimations	Error, %
B	25 °C	26.32	26.3148	0.0198
S10		27.23	27.2296	0.0015
S20		32.01	32.0112	0.0037
S30*		33.65	33.6472	0.0083
S40		30.59	30.5911	0.0036
B		60 °C	24.03	24.018
S10	25.27		25.2658	0.0166
S20	29.67		29.7121	0.1419
S30*	31.28		31.2765	0.0112
S40	28.09		28.0675	0.0801
B	80 °C		20.01	20.0075
S10		19.84	19.8314	0.0433
S20		24.88	24.8847	0.0189
S30*		27.09	27.0826	0.0273
S40		24.02	24.0321	0.0504
B		100 °C	12.54	12.5411
S10	16.23		16.2272	0.0173
S20	17		17.012	0.0706
S30*	19.06		19.0562	0.0199
S40	15.88		15.857	0.1448

Note: * Indicates samples used for model testing.

NN validation (effect of 20-minute thermal aging). Table 4 presents the NN prediction results for the DS of the studied samples subjected to 20-minute thermal aging at various temperatures.

Table 4

Experimental and NN results for the dielectric strength of SiR-based composite samples (effect of 20-minute thermal aging)

Sample	$T, ^\circ\text{C}$	Dielectric strength, kV/mm		
		Experimental results	NN estimations	Error, %
B	25 °C	25.01	25.012	0.0080
S10		26.1	26.1014	0.0054
S20		30.5	30.521	0.0689
S30*		32.39	32.387	0.0093
S40		29.37	29.371	0.0034
B		60 °C	20.44	20.438
S10	21.19		21.1903	0.0014
S20	25.47		25.4712	0.0047
S30*	27.77		27.772	0.0072
S40	24.78		24.7835	0.0141
B	80 °C		15.01	15.013
S10		18.89	18.8874	0.0138
S20		19.78	19.7801	0.0005
S30*		21.66	21.6622	0.0102
S40		18.27	18.266	0.0219
B		100 °C	10	10.0034
S10	14.02		14.0201	0.0007
S20	15.49		15.4912	0.0077
S30*	17.62		17.622	0.0114
S40	14.36		14.3613	0.0091

Note: * Indicates samples used for model testing.

The trained NN model effectively estimated the DS values, with prediction errors ranging from 0.0005 % (S20 at 80 °C) to 0.0689 % (S20 at 25 °C).

NN validation (effect of 30-minute thermal aging). Finally, Table 5 summarizes the performance of the NN model in predicting the DS of samples subjected to 30-minute thermal aging. The model demonstrated high

predictive accuracy, with errors ranging from 0.0015 % for sample S20 at 25 °C to 1.0988 % for sample B at 100 °C.

Table 5

Experimental and NN results for the dielectric strength of SiR-based composite samples (effect of 30-minute thermal aging)

Sample	T, °C	Dielectric strength, kV/mm		
		Experimental results	NN estimations	Error, %
B	25 °C	21.52	21.5204	0.0019
S10		22.44	22.4411	0.0049
S20		26.59	26.5904	0.0015
S30*		29	29.0031	0.0107
S40		25.09	25.085	0.0199
B	60 °C	16	16.0012	0.0075
S10		20.11	20.101	0.0448
S20		21.13	21.1364	0.0303
S30*		23.09	23.0881	0.0082
S40		20.45	20.285	0.8068
B	80 °C	14	14.152	1.0857
S10		17.77	17.7864	0.0923
S20		18.59	18.48	0.5917
S30*		20.59	20.5865	0.0170
S40		17.3	17.3021	0.0121
B	100 °C	9.11	9.2101	1.0988
S10		13	13.001	0.0077
S20		14.61	14.6082	0.0123
S30*		16.64	16.5723	0.4069
S40		13.43	13.425	0.0372

Note: * Indicates samples used for model testing.

Conclusions.

1. Experimental studies conducted at four temperature levels (25 °C, 60 °C, 80 °C, and 100 °C) revealed an enhancement in the dielectric strength of the silicone rubber (SiR)-based composites filled with micron-sized silicon dioxide (SiO₂) particles, in comparison to the unfilled (pure) SiR sample.

2. The optimal dielectric strength was observed at a filler concentration of 30 wt %. Beyond this concentration, the dielectric strength declined, possibly due to the formation of conduction channels between filler particles within the SiR matrix.

3. The neural network technique accurately predicted the dielectric strength of SiR insulation filled with micron-sized silicon dioxide. This approach significantly reduced the costs associated with extensive testing and material procurement.

Acknowledgements. The authors express all their gratitude to the staff of the Department of Electrical Engineering, Aswan University, National Research Centre, Department of Polymers and Dyes, and Electrical Voltage Laboratory, where all the samples were made, and experimentations were carried out.

Conflict of interest. The authors declare that they have no conflicts of interest.

REFERENCES

- Rihan M., Sayed A., Abdel-Rahman A.B., Ebeed M., Alghamdi T.A.H., Salama H.S. An artificial gorilla troops optimizer for stochastic unit commitment problem solution incorporating solar, wind, and load uncertainties. *PLOS ONE*, 2024, vol. 19, no. 7, art. no. e0305329. doi: <https://doi.org/10.1371/journal.pone.0305329>.
- Bakeer A., Magdy G., Chub A., Jurado F., Rihan M. Optimal Ultra-Local Model Control Integrated with Load Frequency Control of Renewable Energy Sources Based Microgrids. *Energies*, 2022, vol. 15, no. 23, art. no. 9177. doi: <https://doi.org/10.3390/en15239177>.
- Rashad A., Kamel S., Jurado F., Rihan M., Ebeed M. Optimal design of SSSC and crowbar parameters for performance enhancement

- of Egyptian Zafrana wind farm. *Electrical Engineering*, 2022, vol. 104, no. 3, pp. 1441-1457. doi: <https://doi.org/10.1007/s00202-021-01397-0>.
- Rihan M., Nasrallah M., Hasanin, B. Performance analysis of grid-integrated brushless doubly fed reluctance generator-based wind turbine: modelling, control and simulation. *SN Applied Sciences*, 2020, vol. 2, no. 1, art. no. 114. doi: <https://doi.org/10.1007/s42452-019-1907-0>.
- Noureldeen O., Rihan M., Hasanin B. Stability improvement of fixed speed induction generator wind farm using STATCOM during different fault locations and durations. *Ain Shams Engineering Journal*, 2011, vol. 2, no. 1, pp. 1-10. doi: <https://doi.org/10.1016/j.asej.2011.04.002>.
- Ghazzaly A., Nasrat L., Ebnalwaled K., Rihan M. Recent Advances in Strengthening Electrical, Mechanical and Thermal Properties of Epoxy-Based Insulators for Electrical Applications. *SVU-International Journal of Engineering Sciences and Applications*, 2024, vol. 5, no. 2, pp. 153-161. doi: <https://doi.org/10.21608/svusrc.2024.284150.1216>.
- El Sherkawy E., Nasrat L.S., Rihan M. The effect of thermal ageing on electrical and mechanical properties of thermoplastic nanocomposite insulation of power high-voltage cables. *Electrical Engineering & Electromechanics*, 2024, no. 3, pp. 66-71. doi: <https://doi.org/10.20998/2074-272X.2024.3.09>.
- Sherkawy E.E., Nasrat L.S., Rihan M. Electrical and Mechanical Performances for Low-Density Polyethylene Nano Composite Insulators. *South Asian Research Journal of Engineering and Technology*, 2024, vol. 6, no. 2, pp. 53-60. doi: <https://doi.org/10.36346/sarjet.2024.v06i01.007>.
- Rihan M., Ahmed Z., Nasrat L.S. Advancing High-Voltage Polymeric Insulators: A Comprehensive Review on the Impact of Nanotechnology on Material Properties. *SVU-International Journal of Engineering Sciences and Applications*, 2025, vol. 6, no. 1, pp. 93-105. doi: <https://doi.org/10.21608/svusrc.2025.337910.1250>.
- Rihan M., Hassan A., Ebnalwaled K., Nasrat L.S. Electrical Insulators Based on Polymeric Materials: Toward New Cutting-edge Enhancements. *SVU-International Journal of Engineering Sciences and Applications*, 2025, vol. 6, no. 1, pp. 86-92. doi: <https://doi.org/10.21608/svusrc.2025.311186.1233>.
- Nzenwa E., Adebayo A. Analysis of insulators for distribution and transmission networks. *American Journal of Engineering Research (AJER)*, 2019, vol. 8, pp. 138-145.
- Haque S.M., Ardila-Rey J.A., Umar Y., Mas'ud A.A., Muhammad-Sukki F., Jume B.H., Rahman H., Bani N.A. Application and Suitability of Polymeric Materials as Insulators in Electrical Equipment. *Energies*, 2021, vol. 14, no. 10, art. no. 2758. doi: <https://doi.org/10.3390/en14102758>.
- Ashokrao Fuke C., Anna Mahanwar P., Ray Chowdhury S. Modified ethylene-propylene-diene elastomer (EPDM)-contained silicone rubber/ethylene-propylene-diene elastomer (EPDM) blends: Effect of composition and electron beam crosslinking on mechanical, heat shrinkability, electrical, and morphological properties. *Journal of Applied Polymer Science*, 2019, vol. 136, no. 29, art. no. 47787. doi: <https://doi.org/10.1002/app.47787>.
- Zhu Y. Influence of corona discharge on hydrophobicity of silicone rubber used for outdoor insulation. *Polymer Testing*, 2019, vol. 74, pp. 14-20. doi: <https://doi.org/10.1016/j.polymertesting.2018.12.011>.
- Chudnovsky B.H. *Transmission, distribution, and renewable energy generation power equipment: Aging and life extension techniques*. CRC Press, 2017. 677 p. doi: <https://doi.org/10.1201/9781315152790>.
- Hollaway L.C. Advanced Fiber Reinforced Polymer Composites. *High-Performance Construction Materials: Science and Applications*, 2008, pp. 207-263. doi: https://doi.org/10.1142/9789812797360_0005.
- Ghassemi M. Accelerated insulation aging due to fast, repetitive voltages: A review identifying challenges and future research needs. *IEEE Transactions on Dielectrics and Electrical Insulation*, 2019, vol. 26, no. 5, pp. 1558-1568. doi: <https://doi.org/10.1109/TDEI.2019.008176>.
- Ramalla I., Gupta R.K., Bansal K. Effect on superhydrophobic surfaces on electrical porcelain insulator, improved technique at polluted areas for longer life and reliability. *International Journal of Engineering & Technology*, 2015, vol. 4, no. 4, art. no. 509. doi: <https://doi.org/10.14419/ijet.v4i4.5405>.
- Pandey J.C., Singh M. Dielectric polymer nanocomposites: Past advances and future prospects in electrical insulation perspective. *SPE Polymers*, 2021, vol. 2, no. 4, pp. 236-256. doi: <https://doi.org/10.1002/pls2.10059>.
- Meyer L., Jayaram S., Cherney E.A. Thermal conductivity of filled silicone rubber and its relationship to erosion resistance in the inclined plane test. *IEEE Transactions on Dielectrics and Electrical Insulation*,

- 2004, vol. 11, no. 4, pp. 620-630. doi: <https://doi.org/10.1109/TDEI.2004.1324352>.
21. Zha J.-W., Dang Z.-M., Li W.-K., Zhu Y.-H., Chen G. Effect of micro-Si₃N₄-nano-Al₂O₃ co-filled particles on thermal conductivity, dielectric and mechanical properties of silicone rubber composites. *IEEE Transactions on Dielectrics and Electrical Insulation*, 2014, vol. 21, no. 4, pp. 1989-1996. doi: <https://doi.org/10.1109/TDEI.2014.004330>.
22. Zha J.-W., Zhu Y.-H., Li W.-K., Bai J., Dang Z.-M. Low dielectric permittivity and high thermal conductivity silicone rubber composites with micro-nano-sized particles. *Applied Physics Letters*, 2012, vol. 101, no. 6, art. no. 062905. doi: <https://doi.org/10.1063/1.4745509>.
23. Ramirez I., Cherney E., Jarayam S. Silicone rubber and EPDM micro composites filled with silica and ATH. *2011 Annual Report Conference on Electrical Insulation and Dielectric Phenomena*, 2011, pp. 20-23. doi: <https://doi.org/10.1109/CEIDP.2011.6232586>.
24. Saman N.M., Ahmad M.H., Buntat Z. Application of Cold Plasma in Nanofillers Surface Modification for Enhancement of Insulation Characteristics of Polymer Nanocomposites: A Review. *IEEE Access*, 2021, vol. 9, pp. 80906-80930. doi: <https://doi.org/10.1109/ACCESS.2021.3085204>.
25. Ansoorge S., Schmuck F., Papailiou K. Impact of different fillers and filler treatments on the erosion suppression mechanism of silicone rubber for use as outdoor insulation material. *IEEE Transactions on Dielectrics and Electrical Insulation*, 2015, vol. 22, no. 2, pp. 979-988. doi: <https://doi.org/10.1109/TDEI.2015.7076799>.
26. Suchitra M., Vinay B.K., Parameshwara S., Umashankar M., Panchami S.V. Effect of Combining Nano- and Microfillers for the Assessment of Thermal Class of Glass Fiber-Reinforced Epoxy Composites for Outdoor Insulation. *IEEE Transactions on Dielectrics and Electrical Insulation*, 2023, vol. 30, no. 6, pp. 2896-2904. doi: <https://doi.org/10.1109/TDEI.2023.3285860>.
27. Lokanathan M., Acharya P.V., Ouroua A., Strank S.M., Hebner R.E., Bahadur V. Review of Nanocomposite Dielectric Materials With High Thermal Conductivity. *Proceedings of the IEEE*, 2021, vol. 109, no. 8, pp. 1364-1397. doi: <https://doi.org/10.1109/JPROC.2021.3085836>.
28. Du G., Wang J., Liu Y., Yuan J., Liu T., Cai C., Luo B., Zhu S., Wei Z., Wang S., Nie S. Fabrication of Advanced Cellulosic Triboelectric Materials via Dielectric Modulation. *Advanced Science*, 2023, vol. 10, no. 15, art. no. 2206243. doi: <https://doi.org/10.1002/advs.202206243>.
29. Niu H., Ren Y., Guo H., Małycha K., Orzechowski K., Bai S.-L. Recent progress on thermally conductive and electrical insulating rubber composites: Design, processing and applications. *Composites Communications*, 2020, vol. 22, art. no. 100430. doi: <https://doi.org/10.1016/j.coco.2020.100430>.
30. Bjellheim P., Helgee B. AC breakdown strength of aromatic polymers under partial discharge reducing conditions. *IEEE Transactions on Dielectrics and Electrical Insulation*, 1994, vol. 1, no. 1, pp. 89-96. doi: <https://doi.org/10.1109/94.300236>.
31. Ieda M. Dielectric Breakdown Process of Polymers. *IEEE Transactions on Electrical Insulation*, 1980, vol. EI-15, no. 3, pp. 206-224. doi: <https://doi.org/10.1109/TEI.1980.298314>.
32. Helgee B., Bjellheim P. Electric breakdown strength of aromatic polymers: dependence on film thickness and chemical structure. *IEEE Transactions on Electrical Insulation*, 1991, vol. 26, no. 6, pp. 1147-1152. doi: <https://doi.org/10.1109/14.108152>.
33. Bezprozvannykh G.V., Grynyshyna M.V. Effective parameters of dielectric absorption of polymeric insulation with semiconductor coatings of power high voltage cables. *Electrical Engineering & Electromechanics*, 2022, no. 3, pp. 39-45. doi: <https://doi.org/10.20998/2074-272X.2022.3.06>.
34. Zolotaryov V.M., Chulieieva O.V., Chulieiev V.L., Kuleshova T.A., Suslin M.S. Influence of doping additive on thermophysical and rheological properties of halogen-free polymer composition for cable insulation and sheaths. *Electrical Engineering & Electromechanics*, 2022, no. 2, pp. 35-40. doi: <https://doi.org/10.20998/2074-272X.2022.2.06>.
35. Gurin A.G., Golik O.V., Zolotaryov V.V., Antonets S.Y., Shehebeniuk L.A., Grechko O.M. A statistical model of monitoring of insulation breakdown voltage stability in the process of enameled wires production. *Electrical Engineering & Electromechanics*, 2019, no. 1, pp. 46-50. doi: <https://doi.org/10.20998/2074-272X.2019.1.08>.
36. Shanmuganathan S., Samarasinghe S. *Artificial Neural Network Modelling*. Springer International Publishing, 2016. 472 p. doi: <https://doi.org/10.1007/978-3-319-28495-8>.
37. Kalogirou S.A. Artificial neural networks in renewable energy systems applications: a review. *Renewable and Sustainable Energy Reviews*, 2001, vol. 5, no. 4, pp. 373-401. doi: [https://doi.org/10.1016/S1364-0321\(01\)00006-5](https://doi.org/10.1016/S1364-0321(01)00006-5).
38. Abdolrasol M.G.M., Hussain S.M.S., Ustun T.S., Sarker M.R., Hannan M.A., Mohamed R., Ali J.A., Mekhilef S., Milad A. Artificial Neural Networks Based Optimization Techniques: A Review. *Electronics*, 2021, vol. 10, no. 21, art. no. 2689. doi: <https://doi.org/10.3390/electronics10212689>.
39. Lothongkam C. *Dielectric Strength Behaviour and Mechanical Properties of Transparent Insulation Materials Suitable to Optical Monitoring of Partial Discharges*. Dr.-Ing. Dissertation. Leibniz University Hannover, 2014. 154 p.
40. ASTM D149-09. *Standard Test Method for Dielectric Breakdown Voltage and Dielectric Strength of Solid Electrical Insulating Materials at Commercial Power Frequencies*. 2013, 13 p. doi: <https://doi.org/10.1520/D0149-09>.
41. Essawi S., Nasrat L., Ismail H., Asaad J. Improvement of dielectric strength and properties of cross-linked polyethylene using nano filler. *International Journal of Electrical and Computer Engineering (IJECE)*, 2022, vol. 12, no. 3, pp. 2264-2272. doi: <https://doi.org/10.11591/ijece.v12i3.pp2264-2272>.
42. Ullah I., Akbar M. Anti-aging characteristics of RTV-SiR aided HV insulator coatings: Impact of DC polarity and fillers. *Materials Chemistry and Physics*, 2022, vol. 278, art. no. 125634. doi: <https://doi.org/10.1016/j.matchemphys.2021.125634>.
43. Pleša I., Nožinger P., Schlögl S., Sumereder C., Muhr M. Properties of Polymer Composites Used in High-Voltage Applications. *Polymers*, 2016, vol. 8, no. 5, art. no. 173. doi: <https://doi.org/10.3390/polym8050173>.
44. Laurent C., Teyssedre G., Le Roy S., Baudoin F. Charge dynamics and its energetic features in polymeric materials. *IEEE Transactions on Dielectrics and Electrical Insulation*, 2013, vol. 20, no. 2, pp. 357-381. doi: <https://doi.org/10.1109/TDEI.2013.6508737>.
45. Danikas M.G., Tanaka T. Nanocomposites-a review of electrical treeing and breakdown. *IEEE Electrical Insulation Magazine*, 2009, vol. 25, no. 4, pp. 19-25. doi: <https://doi.org/10.1109/MEI.2009.5191413>.
46. Vinod P., Desai B.M.A., Sarathi R., Kornhuber S. Investigation on the thermal properties, space charge and charge trap characteristics of silicone rubber nano-micro composites. *Electrical Engineering*, 2021, vol. 103, no. 3, pp. 1779-1790. doi: <https://doi.org/10.1007/s00202-020-01195-0>.
47. Basheer I.A., Hajmeer M. Artificial neural networks: fundamentals, computing, design, and application. *Journal of Microbiological Methods*, 2000, vol. 43, no. 1, pp. 3-31. doi: [https://doi.org/10.1016/S0167-7012\(00\)00201-3](https://doi.org/10.1016/S0167-7012(00)00201-3).
48. Ciresan D.C., Meier U., Masci J., Gambardella L.M., Schmidhuber J. Flexible, high performance convolutional neural networks for image classification. *Proceedings of the Twenty-Second International Joint Conference on Artificial Intelligence*, 2011, pp. 1237-1242. doi: <https://doi.org/10.5591/978-1-57735-516-8/IJCAI11-210>.

Received 02.10.2024

Accepted 30.12.2024

Published 02.05.2025

Zahraa Ahmed¹, PhD, Projects Design Engineering,

Loai S. Nasrat², Professor,

Mahmoud Rihan³, Associate Professor,

¹ Department of Projects Design Engineering,

Upper Egypt Electricity Distribution Company, Luxor, Egypt,

e-mail: zahraabelkareem92@gmail.com (Corresponding Author)

² Electrical Power and Machines Engineering Department,

Faculty of Engineering, Aswan University, Egypt,

e-mail: loainasrat@aswu.edu.eg

³ Electrical Power and Machines Engineering Department,

Faculty of Engineering, South Valley University, Qena, Egypt,

e-mail: mahmoudrihan@eng.svu.edu.eg

How to cite this article:

Ahmed Z., Nasrat L.S., Rihan M. The effect of SiO₂ microparticle concentration on the electrical and thermal properties of silicone rubber for electrical insulation applications. *Electrical Engineering & Electromechanics*, 2025, no. 3, pp. 84-89. doi: <https://doi.org/10.20998/2074-272X.2025.3.12>